be expected for a superexchange pathway of the sort found here.

Conclusions

We have shown that under acidic aqueous conditions, reaction between adenine and copper(II) produces several complexes. These include, in addition to the previously reported linear trimer $(AdH^+)_2Cu_3Cl_8 \cdot 4H_2O$, monomeric $(AdH_2^{2+})_2CuCl_6$, dimeric $(Ad)CuCl_2$, and linear-chain polymeric $(AdH^+)_2CuCl_4$. When considered in light of the previously known complexes of copper(II) with both neutral and anionic adenine, the remarkable versatility of multifunctional ligands such as adenine becomes clear.

Acknowledgment. Work at the University of Vermont was supported by the Office of Naval Research. Work performed at the University of North Carolina was supported by the National Science Foundation through Grant No. MPS74-11495-A02 and by the U.S. Public Health Service through Research Grant No. CA15171-03.

Registry No. $(Ad)CuCl_2$, 63904-13-2; $(AdH_2^{2+})_2CuCl_6$, 63904-14-3; $[CuCl_2(AdH^+)_2]Cl_2$, 63915-16-2; $[CuBr_2(AdH^+)_2]Br_2$, 63975-72-4; $(AdH^+)_2Cu_3Cl_8$, 40906-58-9.

Supplementary Material Available: A listing of observed and calculated structure amplitudes for $[CuCl_2(AdH)_2]Cl_2$ (12 pages). Ordering information is given on any current masthead page.

References and Notes

(1) (a) University of Vermont; (b) University of North Carolina.
(2) V. H. Crawford, H. W. Richardson, J. R. Wasson, D. J. Hodgson, and W. E. Hatfield, *Inorg Chem.*, **15**, 2107 (1976), and references therein.
(3) J. A. Carrabine and M. Sundaralingam, *J. Am. Chem. Soc.*, **92**, 369 (1970).
(4) J. F. Villa, *Inorg. Chem.*, **12**, 2054 (1973).
(5) D. B. Brown, J. R. Wasson, J. W. Hall, and W. E. Hatfield, *Inorg. Chem.*, submitted for publication.
(6) The following abbreviations will be used throughout this paper: Ad = neutral adenine, $C_5N_5H_5$; AdH^+ = monoprotonated adenine, $C_5N_5H_6$; AdH_2^{2+} = diprotonated adenine, $C_5N_5H_6$; and $ad\text{-}H^-$ = deprotonated adenine, $C_5H_5H_4$.
(7) S. Foner, *Rev. Sci Instrum.*, **30**, 548 (1959).
(8) D. B. Losee and W. E. Hatfield, *Phys. Rev. B*, **10**, 212 (1974).
(9) E. König, "Magnetic Properties of Transition Metal Compounds", Springer-Verlag, Berlin, 1966.
(10) P. de Meester and A. C. Skapski, *J. Chem. Soc., Dalton Trans.*, 424 (1973).
(11) P. W. R. Corfield, R. J. Doedens, and J. A. Ibers, *Inorg. Chem.*, **6**, 197 (1967).
(12) For a description of the programs used in this analysis, see D. L. Lewis and D. J. Hodgson, *Inorg. Chem.*, **13**, 143 (1974).
(13) The definitions used are $R_1 = \sum[|F_o| - |F_c|]/\sum|F_o|$ and $R_2 = [\sum w(|F_o| - |F_c|)^2/\sum w(F_o)^2]^{1/2}$, where the weights w are $4F_o/\sigma^2(F_o^2)$.
(14) W. H. Zachariasen, *Acta Crystallogr., Sect. A*, **24**, 212 (1968).
(15) Supplementary material.
(16) D. J. Hodgson, *Prog. Inorg. Chem.*, **23**, in press.
(17) H. G. Ringertz, "The Purines-Theory and Experiment", E. D. Bergmann and B. Pullman, Ed., Israel Academy of Science and Humanities, Jerusalem, 1972, pp 61–72.
(18) L. Pauling, "The Nature of the Chemical Bond", 3rd ed, Cornell University Press, Ithaca, N.Y., 1960, p 260.
(19) W. E. Hatfield and E. R. Jones, Jr., *Inorg. Chem.*, **9**, 1502 (1970).
(20) E. Sletten, *Acta Crystallogr., Sect. B*, **25**, 1480 (1969).
(21) A. Terzis, A. L. Beauchamp, and R. Rivest, *Inorg. Chem.*, **12**, 1166 (1973).
(22) P. de Meester and A. C. Skapski, *J. Chem. Soc. A*, 2167 (1971).
(23) R. W. Dyerst, S. J. Baum, and G. F. Kokoszka, *Nature (London)*, **222**, 665 (1969).
(24) D. M. L. Goodgame and K. H. Price, *Nature (London)*, **220**, 783 (1968).
(25) T. Asakawa, M. Inoue, K. Hara, and M. Kubo, *Bull. Chem. Soc. Jpn.*, **45**, 1054 (1972).
(26) M. V. Hanson, C. B. Smith, G. D. Simpson, and G. O. Carlisle, *Inorg. Nucl. Chem. Lett.*, **11**, 225 (1975).
(27) K. Tomita, T. Izuno, and F. Fujiwara, *Biochem. Biophys. Res. Commun.*, **54**, 96 (1973).
(28) T. J. Kistenmacher, L. G. Marzilli, and D. J. Szalda, *Acta Crystallogr., Sect. B*, **32**, 186 (1976).
(29) P. de Meester and A. C. Skapski, *J. Chem. Soc., Dalton Trans.*, 2400 (1972).
(30) R. Weiss and H. Venner, *Hoppe-Seyler's Z. Physiol. Chem.*, **333**, 169 (1963).
(31) B. Bleaney and K. Bowers, *Proc. R. Soc. London, Ser. A*, **214**, 451 (1952).
(32) D. B. Brown, J. A. Donner, J. W. Hall, and W. E. Hatfield, to be sumitted.
(33) E. D. Estes, W. E. Estes, W. E. Hatfield, and D. J. Hodgson, *Inorg. Chem.*, **14**, 106 (1975).
(34) G. Marcotrigiano, L. Menabue, and G. C. Pellacani, *Inorg. Chem.*, **15**, 2333 (1976).
(35) D. J. Hodgson, P. K. Hale, and W. E. Hatfield, *Inorg. Chem.*, **10**, 1061 (1971).
(36) D. B. Brown and W. E. Hatfield, unpublished observations.
(37) J. C. Bonner and M. E. Fisher, *Phys. Rev. A*, **135**, 640 (1964).
(38) M. E. Fisher, *J. Math. Phys. (N.Y.)*, **4**, 124 (1963).
(39) R. W. Jotham, *J. Chem. Soc., Chem. Commun.*, 178 (1973).
(40) D. B. Losee, H. W. Richardson, and W. E. Hatfield, *J. Chem. Phys.*, **59**, 3600 (1973).
(41) J. W. Hall, W. E. Estes, and W. E. Hatfield, to be submitted.

Contribution from the Departments of Chemistry and Physics, Vanderbilt University, Nashville, Tennessee 37235

Structure of Potassium Lead Hexanitrocuprate(II) at 276 K. An Apparent Compressed Tetragonal Jahn–Teller Distortion

MELVIN D. JOESTEN,*[1a] SHOZO TAKAGI,[1a] and P. GALEN LENHERT*[1b]

Received March 2, 1977 AIC701609

Structural data are reported for the orthorhombic phase *Fmmm* of $K_2PbCu(NO_2)_6$. The unit cell contains four formula units and has dimensions of $a = 10.741$ (1), $b = 10.734$ (1), and $c = 10.538$ (1) Å. Intensity data were collected with Mo Kα radiation at 276 K on a four-circle computer-controlled diffractometer. The data set included 1291 observed reflections out to a 2θ limit of 90°. These data were refined by full-matrix least squares to $R = 0.062$. The crystallographic site symmetry for Cu(II) is D_{2h} (*mmm*), but two of the three pairs of Cu–N distances are equal within experimental error. This gives Cu(II) a compressed tetragonal environment with two short Cu–N bonds of 2.058 (9) Å and four long Cu–N bonds with an average distance of 2.160 (10) Å. Comparisons are made with structural results for five other compounds in the $M_2M'Cu(NO_2)_6$ series and three compounds in the $K_2M'Ni(NO_2)_6$ series. Arguments are presented which suggest that the compressed tetragonal CuN_6 configuration in statically distorted $M_2PbCu(NO_2)_6$ compounds is a dynamic average of two elongated tetragonal CuN_6 groups.

Introduction

Recent x-ray diffraction studies in our laboratory indicate that the $M_2M'Cu(NO_2)_6$ series of compounds is ideal for studies of the dynamic–static Jahn–Teller effect. The potential of these compounds for such studies was first recognized by Elliott, Hathaway, and Slade[2] who interpreted a low-temperature isotropic–anisotropic EPR spectral transition for powdered $K_2PbCu(NO_2)_6$ in terms of a dynamic–static Jahn–Teller effect. All $M_2M'Cu(NO_2)_6$ compounds we have investigated either are orthorhombic at 295 K or undergo cubic to orthorhombic phase transitions between 295 and 281 K. At 295 K the CuN_6 configuration is octahedral in $K_2PbCu(N-$

Table I. Lattice Parameters for $K_2PbCu(NO_2)_6$ Crystals

Crystal[a]	Temp, K	No. of refln[e]	Cell constants, A		
			a	*b*	*c*
1 and 2 (av)	193	25	10.722 (3)	10.742 (4)	10.508 (3)
3	278	18	10.733 (3)	10.737 (3)	10.538 (3)
	268	28	10.737 (4)	10.746 (4)	10.517 (4)
4[b]	276	15	10.741 (1)	10.734 (1)	10.538 (1)
5	277	15	(*c*) 10.739 (2)	10.734 (2)	10.535 (2)
			(*d*) 10.735 (1)	10.732 (1)	10.541 (1)
	268	13	10.750 (4)	10.734 (3)	10.518 (3)
6	278	13	10.740 (3)	10.731 (2)	10.532 (3)
7	295	15	10.6747 (6)		
	278	12	10.729 (2)	10.734 (2)	10.540 (1)
	268	12	(*c*) 10.730 (4)	10.739 (4)	10.519 (4)
			(*d*) 10.735 (3)	10.750 (3)	10.520 (3)

[a] The unresolved Mo Kα doublet (0.710 69 Å) was used for crystals 1 and 2. All other lattice measurements listed were made with the resolved Cu $K\alpha_1$ line (1.540 51 Å). [b] Crystal used for data collection. [c] Prominent lattice. [d] Although all crystals had several lattices present, accurate lattice parameter measurements were possible for a second lattice in only a few instances where the intensities were almost as strong as those in the first lattice. [e] $48 < 2\theta < 72°$ for all reflections used except for crystals 1 and 2 where $26 < 2\theta < 39°$.

$O_2)_6$[3,4] and $Tl_2PbCu(NO_2)_6$,[5] compressed tetragonal in $Rb_2PbCu(NO_2)_6$,[6] and elongated tetragonal in $K_2CaCu(NO_2)_6$,[7] $K_2SrCu(NO_2)_6$,[8] and $K_2BaCu(NO_2)_6$.[9] Corresponding $M_2M'Ni(NO_2)_6$ compounds are cubic over the temperature range 130–295 K.

Low-temperature single-crystal EPR and x-ray powder studies by Harrowfield and co-workers[10,11] on $K_2PbCu(NO_2)_6$ and $Tl_2PbCu(NO_2)_6$ were interpreted in terms of two tetragonal phase transitions which were observed at 281 and 273 K for $K_2PbCu(NO_2)_6$[10] and at 291 and 245 K for $Tl_2PbCu(NO_2)_6$.[11] We have shown that the low-temperature phases are actually orthorhombic *Fmmm* rather than tetragonal.[7,12] However, the CuN_6 configuration can be discussed in terms of pseudotetragonal symmetry since two of the three pairs of Cu–N bonds are nearly equal within experimental error in all the compounds we have investigated.

In the present report the low-temperature structure of $K_2PbCu(NO_2)_6$ is described, and comparisons are made with x-ray and EPR results for the $M_2M'Cu(NO_2)_6$ series.

Experimental Section

Greenish black crystals of $K_2PbCu(NO_2)_6$ were obtained by the method of Reinen, Friebel, and Reetz.[13] Precession photographs at 240 K showed two or more lattices with one usually more prominent than the others.[7,12] All lattices strong enough to be examined are orthorhombic. The similarity of these precession photographs with those for $K_2CaCu(NO_2)_6$ and $K_2BaCu(NO_2)_6$ at 295 K led us to assume the same orthorhombic space group, *Fmmm*.

Since Harrowfield and Pilbrow[10] had detected phase changes at 281 and 273 K, we decided to obtain lattice parameters for several crystals at low temperature. The lattice parameters listed in Table I and the intensity data for crystal 4 were measured with a four-circle computer-controlled diffractometer. The diffractometer control program is described elsewhere.[14] The temperature was controlled with a Cryogenic Associates Model CT-38 controlled temperature Dewar which has been modified and tested on the diffractometer in our laboratory.[15] The cell constants for each crystal examined were determined from least-squares refinement of 2θ, ω, and χ values (see Table I).

Three-dimensional intensity data were collected at 276 K on crystal 4 of Table I which measured 0.2 × 0.3 × 0.3 mm. θ–2θ scans with Nb-filtered Mo Kα radiation were used for reflections with $2\theta > 12°$ and Zr–Y balanced filters were used for reflections with $2\theta < 12°$. Three monitor reflections showed a negligible decrease in intensity after 117 h of x-ray exposure. Absorption corrections were calculated with the program ORABS[16] using a linear absorption coefficient for Mo Kα of 157.4 cm^{-1} and a Gaussian grid 11 × 11 × 11; maximum and minimum transmission factors were 0.131 and 0.031. All reflections (1300) out to $2\theta = 90°$ in the *hkl* octant and 78 reflections in the $hk\bar{l}$ octant were measured and then combined to give 1291 independent reflections which were all observed ($F_o > 0$). Since several lattices were present, 80 overlapping or coincident reflections at or near the twin boundary[12] were dropped from the data set to eliminate measurement errors caused by reflection overlap. Further details of the data collection and reduction methods have been described previously.[17]

The crystal structure of $K_2PbCu(NO_2)_6$ was refined by using, as starting coordinates, those obtained for isostructural $Rb_2PbCu(NO_2)_6$. In the space group, *Fmmm*, the four copper atoms occupy the special position *a* (*mmm* symmetry) and the four lead atoms, *b* (*mmm*). Special position *f* (222) is occupied by eight potassium atoms; *g*, *h*, and *i* (*mm*) are occupied by 24 nitrogen atoms; and *m*, *n*, and *o* (*m*) are occupied by 48 oxygen atoms. Full-matrix least-squares minimized $\sum w(|F_o| - |F_c|)^2$ where $w = 1/\sigma^2(F_o)$. The variance, σ^2, was based on counting statistics and included the usual instability term (0.69% in this case) determined as described previously.[17] All atoms were refined anisotropically along with the extinction parameters which refined to a value of 0.1734 × 10^{-4} cm for r^* (Zachariasen[18]). Atomic scattering factors for neutral atoms were those tabulated by Cromer and Mann.[19] Anomalous scattering factors were those given by Cromer and Liberman.[20]

The final cycles of full-matrix least squares on 1211 reflections reduced the conventional *R* factor to 0.062 and the weighted *R* factor, $R_w = \{[\sum w(|F_o| - |F_c|)^2]/\sum w|F_o|^2\}^{1/2}$ to 0.062. The standard error of an observation of unit weight was 6.90, the final average and maximum shift-to-error ratios for the atomic parameters are 0.002 and 0.017, respectively, and the maximum and minimum electron densities on the final difference map were 8.0 and −9.0 e/Å^3 near Pb. The positional and thermal parameters and their standard deviations are displayed in Table II. The values shown were used (before rounding) to calculate the final structure factors.[21]

Structure factor, electron density, bond distance and angles, and least-squares calculations were carried out with the X-RAY 67 programs[22] as implemented and updated on the Vanderbilt Sigma 7 computer.

Three-dimensional intensity data were also collected at 193 K on crystal 2 of Table I [a = 10.718 (4), b = 10.743 (5), c = 10.510 (4) Å]. A total of 1240 reflections were measured in the *hkl* octant. The procedures described above were used for data reduction and refinement. A value of 0.081 was obtained for the conventional *R* factor. The poorer-than-expected precision was traced in part to the cryostat mounting bracket which was found to flex, resulting in crystal motion and causing errors in the measured intensities. Bond distances and angles are given in Table III but the atomic parameters are not included.

Table II. Positional and Thermal Parameters for $K_2PbCu(NO_2)_6$ at 276 K

	x	*y*	*z*	B_{11}	B_{22}	B_{33}	B_{12}	B_{13}	B_{23}
Cu	0	0	0	1.04 (5)	0.80 (6)	1.15 (5)			
Pb	0	0	1/2	1.24 (2)	0.91 (2)	1.19 (2)			
K	1/4	1/4	1/4	3.33 (14)	3.05 (17)	3.17 (12)			
O(1)	0	0.0985 (9)	0.2565 (7)	3.77 (31)	1.90 (29)	2.07 (21)			−0.62 (20)
O(2)	0.0988 (7)	0.2622 (9)	0	1.85 (23)	2.93 (39)	4.23 (34)	−0.51 (23)		
O(3)	0.2620 (8)	0	0.0998 (7)	3.09 (32)	2.90 (38)	2.12 (22)		−0.52 (23)	
N(1)	0	0	0.1953 (9)	2.40 (38)	2.27 (45)	1.00 (24)			
N(2)	0	0.2006 (13)	0	1.82 (34)	2.13 (47)	1.77 (30)			
N(3)	0.2017 (13)	0	0	2.41 (45)	0.98 (43)	4.99 (68)			

[a] The thermal parameters are of the form $T = \exp[-1/4(B_{11}h^2a^{*2} + B_{22}k^2b^{*2} + B_{33}l^2c^{*2} + 2B_{12}hka^*b^* + 2B_{13}hla^*c^* + 2B_{23}klb^*c^*)]$.

Table III. Comparison of Bond Distances (Å) and Bond Angles (deg) for Cubic and Orthorhombic Forms of $M_2M'M''(NO_2)_6$ Compounds

	$M_2M'M''$										
Bond	K_2PbNi[a] 295 K	K_2SrNi[b] 295 K	K_2BaNi[c] 295 K	Tl_2Pb-Cu[d] 295 K	K_2PbCu[a] 295 K	K_2PbCu[e] 276 K	K_2PbCu[e] 193 K	Rb_2Pb-Cu[f] 295 K	K_2CaCu[g] 295 K	K_2SrCu[b] 295 K	K_2BaCu[h] 295 K
M''-N(1)	2.080 (2)	2.078 (2)	2.080 (2)	2.118 (6)	2.118 (2)	2.058 (9)	2.071 (14)	2.063 (3)	2.050 (1)	2.041 (2)	2.038 (2)
M''-N(2)						2.153 (14)	2.151 (16)	2.173 (4)	2.313 (1)	2.310 (2)	2.311 (2)
M''-N(3)						2.166 (13)	2.133 (31)	2.173 (4)	2.052 (1)	2.029 (2)	2.048 (2)
N(1)-O(1)	1.245 (2)	1.248 (1)	1.248 (3)	1.252 (4)	1.247 (2)	1.238 (10)	1.206 (12)	1.243 (2)	1.246 (1)	1.242 (1)	1.232 (2)
N(2)-O(2)						1.250 (11)	1.255 (15)	1.240 (3)	1.252 (1)	1.251 (1)	1.236 (2)
N(3)-O(3)						1.234 (10)	1.293 (19)	1.248 (3)	1.246 (1)	1.246 (1)	1.229 (2)
M-O(1)	3.082 (1)	3.060 (1)	3.151 (1)	3.135 (2)	3.116 (1)	3.140 (5)	3.144 (5)	3.169 (1)	3.053 (1)	3.143 (1)	3.203 (1)
M-O(2)						3.097 (4)	3.095 (7)	3.130 (1)	3.011 (1)	3.046 (1)	3.135 (1)
M-O(3)						3.118 (4)	3.094 (5)	3.145 (1)	3.088 (1)	3.106 (1)	3.240 (1)
M'-O(1)	2.773 (2)	2.732 (1)	2.866 (2)	2.802 (3)	2.778 (1)	2.775 (8)	2.787 (11)	2.806 (2)	2.674 (1)	2.753 (1)	2.866 (1)
M'-O(2)						2.765 (9)	2.742 (12)	2.788 (2)	2.610 (1)	2.709 (1)	2.844 (2)
M'-O(3)						2.765 (8)	2.763 (10)	2.785 (2)	2.676 (1)	2.745 (1)	2.875 (2)
O(1)-N(1)-O(1)	117.3 (2)	116.4 (1)	117.2 (2)	116.6 (5)	116.9 (2)	117.2 (9)	120.2 (14)	117.4 (3)	116.6 (1)	117.1 (1)	117.6 (2)
O(2)-N(2)-O(2)						116.2 (12)	114.7 (15)	116.0 (4)	115.2 (1)	115.8 (1)	116.0 (2)
O(3)-N(3)-O(3)						116.8 (12)	114.6 (24)	115.5 (4)	116.7 (1)	116.7 (1)	117.3 (2)

[a] Reference 4. [b] Reference 8. [c] Reference 23. [d] Reference 5. [e] This work. [f] Average of two structural determinations on different crystals, ref 6. [g] Reference 7. [h] Reference 9.

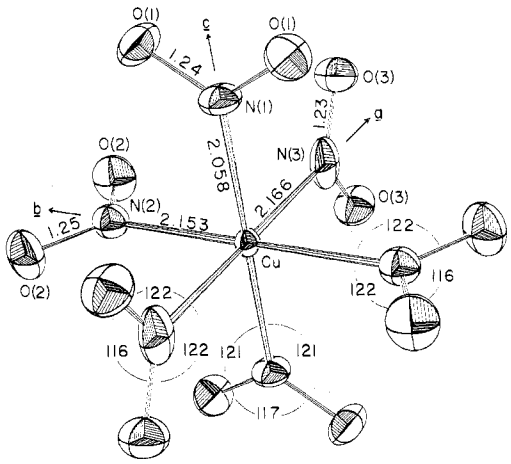

Figure 1. Hexanitrocuprate(II) anion of $K_2PbCu(NO_2)_6$ at 276 K.

Discussion

$K_2PbCu(NO_2)_6$. The configuration of the hexanitrocuprate(II) ion in $K_2PbCu(NO_2)_6$ at 276 K is shown in Figure 1. Bond distances and bond angles are shown in Figure 1 and are listed with standard deviations in Table III. The crystallographic site symmetry for Cu(II) is D_{2h} (*mmm*), but two of the three pairs of Cu–N distances are equal within experimental error. Thus, the CuN_6 configuration is compressed tetragonal with an average Cu–N bond length of 2.160 (10) Å for the long bonds and 2.058 (9) Å for short bonds. The difference between the long and short bonds is identical with the difference of 0.10 Å found for $Rb_2PbCu(NO_2)_6$ at 295 K (Table III).

All crystals of the $M_2M'Cu(NO_2)_6$ series which we have investigated show a tendency to twin in the orthorhombic phase. We have discussed this property previously[7,12] and have provided direct evidence from precession photographs that the lattices have a common {110} boundary which was first proposed for the low-temperature phases of $K_2PbCu(NO_2)_6$ by Harrowfield and Pilbrow.[10] Since the presence of several lattices is in accord with the notion that a dynamic Jahn–Teller distortion can be trapped in a favorable crystal field, the relationship of the lattices to each other is of interest. As reported previously,[12] the angles between the lattice directions of the twins are related directly to the cell constants. This relationship is found whenever the orthorhombic phase is present regardless of whether the CuN_6 configuration is compressed or elongated and the values of the interlattice angles in each case are determined by the unit cell dimensions of the lattice. However, the relative intensities of x-ray reflections from the different lattices vary with crystal, temperature, and applied stress.[10] For those compounds which crystallize in the orthorhombic phase at 295 K, one lattice tends to be more prominent than the others, and usually crystals can be found which show negligible diffraction from the second lattice.[7,9]

The cubic $K_2PbCu(NO_2)_6$ crystals which have been cooled through the cubic to orthorhombic transition to 276 K usually have two lattices with approximately equal intensities and several additional lattices with weak intensities. When the same crystal is further cooled to 268 K, the intensities of the strong lattices generally become weaker presumably due to additional splitting. However, the same effect can be obtained by recycling the temperature through the first phase transition.

We were interested in examining the two phase transitions at 281 and 273 K[10] in order to study the changes in lattice parameters and in relative diffraction intensities. Table I lists lattice parameters for several crystals at low temperatures; all of them are orthorhombic (*Fmmm*). If all measurements made at 276–278 K with Cu $K\alpha_1$ radiation are averaged, one finds a,b = 10.735 Å and c = 10.537 Å where both long cell edges have been combined. The 268 K measurements, treated in the same way, give a,b = 10.740 Å and c = 10.519 Å. These results are in fair agreement with the slightly less accurate values found by Harrowfield and Pilbrow[10] and indicate an expansion of 0.062 Å along a,b with a contraction of 0.136 Å along c for the cubic to orthorhombic transition and a probable further expansion of 0.005 Å along a,b with a further contraction of 0.018 Å along c for the second phase transition. Although a change in lattice constants is unquestionably associated with the second phase transition at 273 K, we are unable to detect an associated structural change. As noted above, the data set for crystal 2 at 193 K was not accurate enough to give precise bond distances, but the Cu–N and other interatomic distances listed in Table III show the same type of compressed tetragonal CuN_6 configuration found at 276 K.

Comparison of $K_2PbCu(NO_2)_6$ and Other $M_2M'M''(NO_2)_6$ Structures. All single-crystal x-ray bond distance and angle results for $M_2M'M''(NO_2)_6$ compounds are displayed in Table III. The results from five cubic forms (three with M'' = Ni and two with M'' = Cu) are shown on the left, followed by three orthorhombic structures with compressed tetragonal CuN_6 groups and, on the right, three orthorhombic structures with elongated tetragonal CuN_6 groups. In the following

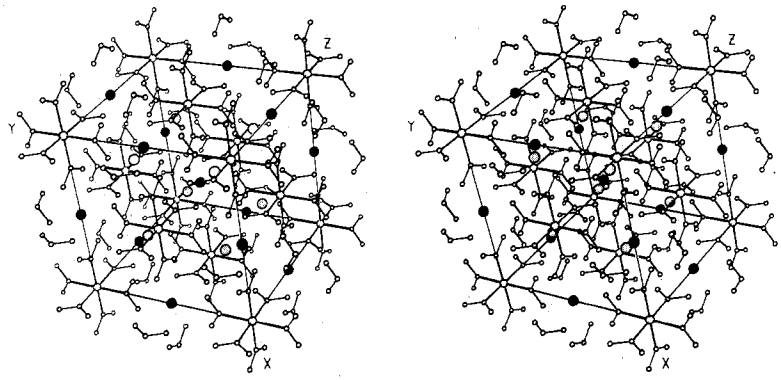

Figure 2. Stereoview of the unit cell and adjacent groups for $Rb_2PbCu(NO_2)_6$: solid circles, Pb^{2+}; stippled circles, Rb^+.

discussion we will point out features of the $Cu(NO_2)_6^{4-}$ cluster and its packing which relate to the particular counterions around it. The compressed structures with M′ = Pb and the elongated structures with M′ = Ca, Sr, or Ba both form particularly interesting series.

M influences the transition temperature from orthorhombic to cubic and M′ determines whether the orthorhombic form will contain an elongated or compressed $Cu(NO_2)_6^{4-}$ cluster. The relationship of M and M′ to the $Cu(NO_2)_6^{4-}$ cluster is shown in the stereoscopic view of the unit cell in Figure 2. (A more detailed discussion of the crystal packing is given in ref 7 and 23). The two principal features of the counterion packing around $Cu(NO_2)_6^{4-}$ are (1) the divalent ions (M′) lie between the $Cu(NO_2)_6^{4-}$ clusters along the line of the Cu–N bonds, and (2) the monovalent cations (M) are located between the layers made up of M′ ions and $Cu(NO_2)_6^{4-}$ ions in a "pocket" surrounded tetrahedrally by four $Cu(NO_2)_6^{4-}$ ions and by four M′ ions.

Although all the $M_2PbCu(NO_2)_6$ compounds listed in Table III contain compressed tetragonal CuN_6 groupings, the counterion, M, does influence the temperature for the cubic to orthorhombic transition. Rb^+, Tl^+, and K^+ in $M_2PbCu(NO_2)_6$ have cubic to orthorhombic transitions at 317, 291, and 281 K, respectively.[6] This correlates with the ionic radii of the ions (Rb^+ = 1.48 Å, Tl^+ = 1.44 Å, K^+ = 1.33 Å). If the differences between the observed M–O distance and the ionic radius of M are compared, the values are 1.668 Å for the Rb^+ salt, 1.695 Å for the Tl^+ salt, and 1.786 Å for the K^+ salt. These distances indicate Rb^+ essentially fills the "M pocket" and is close to contact distance with neighboring oxygen atoms. The smallest ion, K^+, is a loose fit in the "pocket" formed by the $Cu(NO_2)_6^{4-}$ anions.

The three structures exhibiting elongated tetragonal CuN_6 distortions (Table III) show a correlation between the K–O distances, the M′–O distances, and the ionic radius of M′. The average K–O distances to the oxygen atoms of the NO_2 groups with short Cu–N bonds differ in a regular way from the average K–O distances to the oxygen atoms of the NO_2 groups with long Cu–N bonds. As the ionic radius of M′ increases (Ca^{2+}, Sr^{2+}, Ba^{2+}, 0.99, 1.13, 1.35 Å), the difference between K–O distances of the long and short groups [K–O(long) – K–O(short)] increases from 0.056 Å (M′ = Ca^{2+}) to 0.087 Å (M′ = Ba^{2+}). The opposite trend is found if the differences between the M′–O distance for the long and short NO_2 ligands are compared. In this case [M′–O(long) – M′–O(short)] is 0.065 Å for M′ = Ca^{2+} and drops to 0.027 Å for M′ = Ba^{2+}.

A possible explanation for the long and short M′–O distances relates to the residual negative charge carried by the NO_2^- oxygen atoms. The bonding electrons of NO_2^- would be expected to experience a greater shift toward Cu^{2+} in the case of the ligand with the shortest Cu–N bond as compared to the more distant ligand. Therefore, the oxygen atoms on the long Cu–NO_2 moiety will carry a larger formal negative charge than those on the close ligands. The more negative oxygen atoms will bind more closely to M′ and the effect will be larger for Ca^{2+} which has a greater charge to size ratio than Ba^{2+}.

Table IV. A Comparison of Nitrogen Atom "Thermal Motion" for $M_2M'M''(NO_2)_6$ Crystals: Root Mean Square Displacements (Å)[a]

Compd		U_{11}	U_{22}	U_{33}
$K_2PbNi(NO_2)_6$	N(1)	0.130 (3)	0.133 (3)	0.115 (4)*
$K_2SrNi(NO_2)_6$	N(1)	0.120 (2)	0.122 (2)	0.110 (2)*
$K_2BaNi(NO_2)_6$	N(1)	0.140 (4)	*b*	0.118 (3)*
$Tl_2PbCu(NO_2)_6$	N(1)	0.169 (7)	0.149 (7)	0.182 (8)*
$K_2PbCu(NO_2)_6$	N(1)	0.170 (2)	0.164 (2)	0.182 (2)*
$K_2PbCu(NO_2)_6$ (276 K)	N(1)	0.17 (1)	0.17 (2)	0.11 (1)*
	N(2)	0.15 (1)	0.16 (2)*	0.15 (1)
	N(3)	0.18 (2)*	0.11 (2)	0.25 (2)
$Rb_2PbCu(NO_2)_6$[c]	N(1)	0.148 (4)	0.152 (5)	0.128 (5)*
	N(2)	0.182 (5)	0.190 (5)*	0.141 (5)
	N(3)	0.199 (5)*	0.151 (5)	0.144 (5)
$K_2CaCu(NO_2)_6$	N(1)	0.140 (2)	0.120 (2)	0.122 (2)*
	N(2)	0.132 (2)*	0.142 (2)	0.140 (2)
	N(3)	0.130 (2)	0.120 (2)*	0.128 (2)
$K_2SrCu(NO_2)_6$	N(1)	0.141 (3)	0.144 (3)	0.119 (3)*
	N(2)	0.113 (3)*	0.121 (3)	0.138 (3)
	N(3)	0.130 (3)	0.111 (3)*	0.129 (3)
$K_2BaCu(NO_2)_6$	N(1)	0.157 (3)	0.146 (3)	0.122 (3)*
	N(2)	0.138 (3)*	0.158 (3)	0.166 (3)
	N(3)	0.165 (3)	0.121 (3)*	0.142 (3)

[a] Displacements aligned with M″–N bond are indicated with an asterisk. U_{11}, U_{22}, U_{33} are required by symmetry to be aligned with unit cell axes. Literature references are given in Table III. [b] Rotational disorder in NO_2 group, required by symmetry to be equal to U_{11}. [c] Average of two structure determinations on different crystals. See ref 6 for a discussion of possible differences between the two crystals.

The O–N–O angle also correlates with the Cu–N distance. The close ligands have O–N–O angles which are larger than the more distant ligands, an effect observed for both elongated and compressed $Cu(NO_2)_6^{4-}$ clusters. There is also a tendency for the O–N–O angle to open slightly as the M′–O distance increases.

The Cu–N distance in the cubic (dynamic) case is 2.118 Å which is 0.014 Å shorter than the average Cu–N distance found for *all* orthorhombic (static) lattices. Both the compressed and elongated tetragonal cases have an average Cu–N distance of 2.132 Å. We have no explanation for the shorter Cu–N bond in the cubic case. It is surprising that both types of static distortions give the same average Cu–N distance while the average Cu–N distance in the dynamic case shows a significant difference.

The thermal parameters of the $M_2PbCu(NO_2)_6$ series show some interesting differences from those of the $K_2M'Cu(NO_2)_6$ series. Table IV summarizes the relevant thermal motion data from all crystal studies to date of compounds which contain $Cu(NO_2)_6^{4-}$ and $Ni(NO_2)_6^{4-}$ clusters. In nearly all cases the

differences in the root mean square amplitudes are statistically significant. The validity of the observations is further enhanced by the fact that all x-ray data sets were corrected for absorption and isotropic extinction and in most cases symmetry equivalent reflections were combined in the final data set. These precautions should reduce the effect of any systematic errors present in the original x-ray measurements.

Reference to Table IV shows the following. (1) The three crystals with the non-Jahn–Teller $Ni(NO_2)_6^{4-}$ cluster each show a significantly smaller root mean square vibration amplitude along the Ni–N bonds than at right angles to them. (2) The cubic $Cu(NO_2)_6^{4-}$ clusters [both $K_2PbCu(NO_2)_6$ and $Tl_2PbCu(NO_2)_6$] show greater apparent thermal motion *along* the Cu–N bonds than perpendicular to them. (3) The $Cu(NO_2)_6^{4-}$ clusters with elongated tetragonal CuN_6 groups show, with one exception [N(1) of $K_2CaCu(NO_2)_6$], greater root mean square amplitude normal to the Cu–N bonds and smaller amplitudes along the bonds. (4) The two structures with compressed $Cu(NO_2)_6^{4-}$ clusters [$K_2PbCu(NO_2)_6$ at 276 K and $Rb_2PbCu(NO_2)_6$] show root mean square amplitudes similar to the elongated clusters for the short Cu–N bonds (N(1) of Table IV), but the long bonds tend to show the largest root mean square amplitude along the bonds. (The latter effect is clear for the $Rb_2PbCu(NO_2)_6$ structure but is obscured in the less accurate $K_2PbCu(NO_2)_6$ structure.)

Cullen and Lingafelter[3] were the first to make observation (2) in their study of cubic $K_2PbCu(NO_2)_6$. They interpreted this unusual observation in terms of a dynamic Jahn–Teller effect which was averaged in the x-ray experiment to give the CuN_6 group octahedral symmetry with six equal Cu–N bonds. A consequence of this interpretation is that the greater apparent thermal motion along the bonds should be reduced in the lower symmetry forms of $K_2PbCu(NO_2)_6$ and in the orthorhombic forms of other crystals which contain the $Cu(NO_2)_6^{4-}$ cluster. Observation (3) supports this interpretation. The non-Jahn–Teller $Ni(NO_2)_6^{4-}$ cluster would also be expected to show greater apparent thermal motion perpendicular to the Ni–N bonds and a smaller root mean square amplitude along the bond. Observation (1) verifies this. Observation (4) suggests that a dynamic averaging is present in the long bonds of the compressed CuN_6 group.

The observed bond distances in the compressed CuN_6 groups as well as the thermal motion parameters support the hypothesis that the compressed CuN_6 configuration is a dynamic average of two static elongated CuN_6 groups. The short Cu–N bonds in the compressed groups are approximately equal to short Cu–N bonds in the elongated CuN_6 groups. The long Cu–N bonds in the compressed groups are nearly equal to the average of one long and one short Cu–N bond from an elongated CuN_6 group. A phase transition to a lattice characteristic of the elongated CuN_8 configuration would confirm that the compressed forms are simply lower symmetry dynamic forms. To check this, crystals with compressed $Cu(NO_2)_6^{4-}$ clusters were cooled. But no change in the crystal lattice is observed when $Rb_2PbCu(NO_2)_6$ crystals are cooled to 130 K.[6] The $K_2PbCu(NO_2)_6$ lattice also retains the apparent compressed tetragonal CuN_6 configuration to similar temperatures. However, the hypothesis that the compressed configuration is a dynamic average of two orientations of the elongated configuration is supported by EPR measurements as discussed below.

Theoretical expressions for g values are $g_\perp = 2 - (2\lambda/\Delta)$ and $g_\parallel = (2 - 8\lambda)/\Delta$ for Cu(II) in an elongated tetragonal environment and $g_\perp = 2 - (6\lambda/\Delta)$ and $g_\parallel = 2$ for Cu(II) in a compressed tetragonal environment.[24] The average $g_\parallel$ and $g_\perp$ values reported[2,13] for $M_2M'Cu(NO_2)_6$ compounds which are known to contain tetragonally elongated CuN_6 are $g_\parallel$ elongated average = 2.248 and $g_\perp$ elongated average = 2.063. Literature reports of single-crystal g values for $M_2PbCu(NO_2)_6$ compounds which contain tetragonally compressed CuN_6 include $g_\parallel = 2.059$ and $g_\perp = 2.147$ for $K_2PbCu(NO_2)_6$,[10] $g_\parallel = 2.066$, $g_\perp = 2.146$ for $Tl_2PbCu(NO_2)_6$,[11] and $g_\parallel = 2.073$ and $g_\perp = 2.155$ for $Rb_2PbCu(NO_2)_6$.[25] Earlier, Elliott, Hathaway, and Slade[2] had interpreted powder g values of 2.061 and 2.155 for $K_2PbCu(NO_2)_6$ at low temperature as evidence against the presence of a compressed tetragonal distortion since the theoretically predicted value of 2 was not obtained. However, Harrowfield and Pilbrow[10] proposed that vibronic effects may cause the $g_\parallel$ value to be a little larger than 2.

If we consider that the tetragonally compressed CuN_6 configuration found in statically distorted $M_2PbCu(NO_2)_6$ compounds is really a dynamic average of two tetragonally elongated configurations, the single-crystal EPR data listed above could be interpreted as $g_\parallel$ compressed crystal = $g_\perp$ elongated average and $g_\perp$ compressed crystal = $^1/_2(g_\parallel$ elongated average + $g_\perp$ elongated average). Using the average elongated tetragonal values of $g_\perp$ elongated average = 2.063 and $g_\parallel$ elongated average = 2.248 gives $g_\parallel$ compressed crystal = 2.063 and $g_\perp$ compressed crystal = 2.155. These values are in excellent agreement with the single-crystal values listed above for $M_2PbCu(NO_2)_6$ compounds. On the basis of these arguments we suggest that the static distortion in $M_2PbCu(NO_2)_6$ compounds should be labeled pseudocompressed tetragonal.

Since only compounds with $M' = Pb^{2+}$ show the pseudocompressed configuration, it is necessary to ask what differences between Pb^{2+} and alkaline earth ions may influence the structure of the $M_2M'Cu(NO_2)_6$ series. Ionic size is not the determining factor since Sr^{2+} (1.13 Å) and Ba^{2+} (1.35 Å) bracket the ionic size of Pb^{2+} (1.21 Å), and $M_2M'Cu(NO_2)_6$ compounds with $M' = Sr^{2+}$ and Ba^{2+} contain elongated tetragonal $Cu(NO_2)_6^{4-}$ units. Major differences between Pb^{2+} and alkaline earth ions include the presence of a lone pair of electrons in the valence shell of Pb^{2+} and a greater tendency for Pb^{2+} to form covalent bonds.

Structural studies of $Pb[OP(C_6H_5)_2O]_2$,[26] $Pb[(i\text{-}C_3H_7O_2)_2PS_2]_2$,[27] and tetragonal PbO[28,29] have demonstrated that the lone pair of electrons is stereochemically active in accord with the valence-shell electron-pair repulsion (VSEPR) model.[30] The configuration of Pb^{2+} in the first two compounds is close to a pentagonal bipyramid with the lone pair in an equatorial position. In tetragonal PbO the lone pair is postulated to occupy the apex of a tetragonal pyramid.[29] In the present case six NO_2^- ligands surround Pb^{2+} at Pb–O distances (2.78 Å) longer than those found in PbO (2.21, 2.49 Å) or $Pb[OP(C_6H_5)_2O]_2$ (2.233, 2.435 Å). However, the unique ability of Pb^{2+} to give a pseudocompressed tetragonal $Cu(NO_2)_6^{4-}$ configuration in $M_2M'Cu(NO_2)_6$ compounds may be explained by considering the repulsive interactions between the lone pair and the NO_2^- ligands. The most favorable arrangement would be with the lone pair in an sp_z hybrid orbital. (Use of sp_z hybrid orbitals for the "inert" pair of Pb^{2+} was first proposed by Orgel[31] to explain NMR data for a series of Pb^{2+} compounds.) This would give repulsions with two NO_2^- ligands (along the c unit cell axis) rather than four NO_2^- ligands in the *ab* plane. Although such an arrangement would lead to a compressed tetragonal $Cu(NO_2)_6^{4-}$ unit, the distance between Pb^{2+} and NO_2^- ligands is probably too large for sp_z repulsion to be the sole cause of the 0.2 Å shortening in c.

Another possibility is for the lone pair to occupy an equatorial position with a pseudorotational oscillation ("pseudo-Jahn–Teller" effect) similar to that proposed for IF_7.[32] Such an effect would give similar Pb–O distances for the four NO_2^- ligands around Pb^{2+} in the *ab* plane. This "pseudo-Jahn–Teller" effect could account for the larger N

atom thermal motion along the equatorial Cu–N bonds in the static phase of $M_2PbCu(NO_2)_6$ compounds. Since the effect of the lone pair on Pb^{2+} is not seen in the corresponding $K_2PbNi(NO_2)_6$ structure, it is not important enough to affect a non-Jahn–Teller ion similar in size to Cu^{2+}. However, it does appear to be of sufficient importance to influence the type of Jahn–Teller distortion in $M_2M'Cu(NO_2)_6$ compounds.

The other difference between Pb^{2+} and alkaline earth ions is the greater tendency of Pb^{2+} to form covalent bonds. Electronic spectral data provide evidence for electron transfer from Pb^{2+} to the $Cu(NO_2)_6^{4-}$ unit.[33] However, the Pb–O bond is too long for covalent contributions to have an important effect on $Cu(NO_2)_6^{4-}$ geometry. In our opinion, the most important cause of the pseudocompressed tetragonal $Cu(NO_2)_6^{4-}$ is the stereochemical activity of the lone pair of electrons on Pb^{2+}.

Acknowledgment. We wish to acknowledge the helpful suggestions of a referee which clarified the interpretation of the compressed distortion, especially as it relates to the EPR data. Support of this research by the National Science Foundation (GP-38022X) and Vanderbilt University is gratefully acknowledged.

Registry No. $K_2PbCu(NO_2)_6$, 15291-22-2.

Supplementary Material Available: A listing of structure factor amplitudes (3 pages). Ordering information is given on any current masthead page.

References and Notes

(1) (a) Department of Chemistry. (b) Department of Physics.
(2) H. Elliott, B. J. Hathaway, and R. C. Slade, *Inorg. Chem.*, **5**, 669 (1966).
(3) D. L. Cullen and E. C. Lingafelter, *Inorg. Chem.*, **10**, 1264 (1971).
(4) S. Takagi, M. D. Joesten, and P. G. Lenhert, *Acta Crystallogr., Sect. B*, **31**, 1968 (1975).
(5) S. Takagi, M. D. Joesten, and P. G. Lenhert, *Acta Crystallogr., Sect. B*, **32**, 326 (1976).
(6) S. Takagi, M. D. Joesten, and P. G. Lenhert, *J. Am. Chem. Soc.*, **97**, 444 (1975); S. Takagi, M. D. Joesten, and P. G. Lenhert, *Acta Crystallogr., Sect. B*, **32**, 1278 (1976).
(7) S. Takagi, P. G. Lenhert, and M. D. Joesten, *J. Am. Chem. Soc.*, **96**, 6606 (1974).
(8) S. Takagi, M. D. Joesten, and P. G. Lenhert, *Acta Crystallogr., Sect. B*, **32**, 2524 (1976).
(9) S. Takagi, M. D. Joesten, and P. G. Lenhert, *Acta Crystallogr., Sect. B*, **31**, 596 (1975).
(10) B. V. Harrowfield and J. R. Pilbrow, *J. Phys. C*, **6**, 755 (1973).
(11) B. V. Harrowfield, A. J. Dempster, T. E. Freeman, and J. R. Pilbrow, *J. Phys. C*, **6**, 2058 (1973).
(12) S. Takagi, M. D. Joesten, and P. G. Lenhert, *Chem. Phys. Lett.*, **34**, 92 (1975).
(13) D. Reinen, C. Friebel, and K. P. Reetz, *J. Solid State Chem.*, **4**, 103 (1972).
(14) P. G. Lenhert, *J. Appl. Crystallogr.*, **8**, 568 (1975).
(15) P. G. Lenhert and S. Takagi, Paper B19, American Crystallographic Association Meeting, Aug 18–23, 1974.
(16) D. J. Wehe, W. R. Busing, and H. A. Levy, "ORABS, a Fortran Program for Calculating Single-Crystal Absorption Corrections," Oak Ridge National Laboratory Report ORNL-TM-229, Oak Ridge, Tenn., 1962.
(17) P. T. Miller, P. G. Lenhert, and M. D. Joesten, *Inorg. Chem.*, **11**, 2221 (1972).
(18) W. H. Zachariasen, *Acta Crystallogr., Sect. A*, **24**, 212 (1968).
(19) D. T. Cromer and J. B. Mann, *Acta Crystallogr., Sect. A*, **24**, 321 (1968).
(20) D. T. Cromer and D. Liberman, *J. Chem. Phys.*, **53**, 1891 (1970).
(21) Supplementary material.
(22) J. M. Stewart, "X-Ray 67 Program System for X-Ray Crystallography for the Univac 1108, CDC 3600/6600, IBM 360/50, 65, 75, IBM 7094," Technical Report TR-67-58, Computer Science Center, University of Maryland, College Park, Md., 1967.
(23) S. Takagi, M. D. Joesten, and P. G. Lenhert, *Acta Crystallogr., Sect. B*, **31**, 1970 (1975).
(24) C. J. Ballhausen, "Introduction to Ligand Field Theory," McGraw-Hill, New York, N.Y., 1962, p 134.
(25) M. D. Joesten, S. Takagi, and J. H. Venable, Jr., *Chem. Phys. Lett.*, **36**, 536 (1975).
(26) P. Colamarino, P. L. Orioli, W. D. Benzinger, and H. D. Gillman, *Inorg. Chem.*, **15**, 800 (1976).
(27) S. L. Lawton and G. T. Kakotailo, *Inorg. Chem.*, **11**, 363 (1972).
(28) W. J. Moore and L. Pauling, *J. Am. Chem. Soc.*, **63**, 1392 (1941).
(29) A. F. Wells, "Structural Inorganic Chemistry," 3rd ed., Oxford Press, London, 1972, p 903.
(30) R. J. Gillespie, "Molecular Geometry," Van Nostrand Reinhold, London.
(31) L. E. Orgel, *Mol. Phys.*, **1**, 322 (1958).
(32) W. J. Adams, H. B. Thompson, and L. S. Bartell, *J. Chem. Phys.*, **53**, 4040 (1970).
(33) J. C. Barnes, C. S. Duncan, and R. D. Peacock, *J. Chem. Soc., Dalton Trans.*, 1875 (1972).

Contribution from the Anorganisch-Chemisches Institut der Universität Heidelberg, Im Neuenheimer Feld 270, D-6900 Heidelberg 1, West Germany

Crystal and Molecular Structure of $Te_5O_4F_{22}$: *trans*-$F_2Te(OTeF_5)_4$[1]

HANS PRITZKOW* and KONRAD SEPPELT

Received March 18, 1977 AIC70210+

Crystals of $Te_5O_4F_{22}$ are tetragonal, space group $I4_1/a$, with $a = 9.816$ (2) Å, $c = 20.341$ (6) Å, $Z = 4$, $d_{calcd} = 3.795$ g cm^{-3}, and $V = 1959.9$ Å^3. The refinement for 1178 unique reflections (diffractometer data, $F^2 > \sigma(F^2)$) with anisotropic temperature factors for all atoms converged to $R = 0.048$. The structure is built up by $TeF_2(OTeF_5)_4$ molecules, which have $\bar{4}$ symmetry imposed by the lattice. The central tellurium is bonded to four oxygen atoms of the $OTeF_5$ groups and two fluorine atoms in trans position. The bond angles on all tellurium atoms deviate only slightly from the octahedral symmetry. Average bond distances are Te–F = 1.808 (5) Å for the $OTeF_5$ group, Te–F = 1.849 (8) Å for the central octahedron, and Te–O = 1.875 (5) Å.

Introduction

The compound $Te_5O_4F_{22}$ is a minor product of the reaction of $As(OTeF_5)_3$ with elemental fluorine[2] or, as was found later, a product of the fluorination of $Te(OTeF_5)_4$.[3] Among all known oxide fluorides of Te(VI), it is the only one solid at room temperature, mp 72 °C. The stoichiometry $Te_5O_4F_{22}$ allows many structural isomers, and even with the general rules for the bonding in oxide fluorides of Te(VI) that no Te–O double bonds occur and that the environments around all tellurium atoms are octahedral, there are still 12 isomeric molecules possible.[2] The compound $Te_5O_4F_{22}$ follows these general rules. As already described in a short communication,[4] the molecule obtains high symmetry, in fact the highest possible of all structural isomers.

Experimental Section

Tellurium(VI) tetrakis[oxopentafluorotellurate(VI)] difluoride was prepared as described earlier.[2,3] Although the crystals were almost moisture insensitive they were sealed in glass capillaries for the x-ray measurements. The cell parameters were determined from precession photographs and refined with the indexed lines of a Guinier film (Cu $K\alpha_1$ radiation, λ 1.54051 Å, quartz monochromator, calibration substance $Pb(NO_3)_2$, $a = 7.856$ (1) Å). The space group is determined